Original Paper

Cellular Physiology and Biochemistry

Cell Physiol Biochem 2012;29:361-372

Accepted: January 16, 2012

RNA Interference of PARG Could Inhibit the Metastatic Potency of Colon Carcinoma Cells via PI3-Kinase/Akt Pathway

Qiaozhuan Li[1], Ming Li[2], Ya-Lan Wang[1], Nilufer Jasmine Selimah Fauzee[1], Yi Yang[1], Juan Pan[1], Lian Yang[1] and Alexander Lazar[3]

[1]Department of Pathology, Molecular Medicine and Cancer Research Center, Chongqing Medical University, Chongqing, [2]Department of Pathology, The Affiliated Hospital of Stomatology, Chongqing Medical University, Chongqing, [3]Sarcoma Research Centre & Department of Pathology, The University of Texas MD Anderson Cancer Center, Houston, Texas

Key Words

PARG • PARP • shRNA • PI3K/Akt pathway • NF-κB • MMP2 • MMP9 • Metastasis

Abstract

Aims: To investigate the role and mechanism of PARG inhibition of metastatic behavior in colonic carcinoma cells. Methods: We examined the effects of PARG protein knockdown by RNA interference on invasion, migration and matrix adhesion of colon carcinoma cell lines *in vitro* and using a murine *in vivo* model of liver metastasis. Metastasis related genes were detected using mRNA and protein levels. Moreover, LY294002, an Akt phosphorylation inhibitor, was used to determine whether the suppression of metastatic behavior of colon carcinoma cells was mediated by Akt phosphorylation that was confirmed by EMSA. Pyrrolidine dithiocarbamate (PDTC) was used as a selective NFκ-B inhibitor to clarify the relationship between PARG, PARP and NF-κB. Results: PARG protein was undetectable following specific shRNA transfection; mRNA and protein levels of PARP were significantly decreased. PARG-shRNA cells showed high levels of phosphorylated Akt with decreased expression of NF-κB (both total & nuclear), MMP2 and MMP9 However, no additional changes were noted following inhibition of PI3K/Akt pathway by LY294002 in the PARG-shRNA cells; these cells displayed reduced number of liver metastases when characterized in the murine *in vivo* model. Conclusion: PARG knockdown, concomitant with inhibition of PARP, suppressed the metastatic potency of colon carcinoma cells by activation of PI3K/Akt signaling pathway.

Introduction

Poly ADP-ribosylation is an immediate cellular response to certain types of DNA damage, generated either endogenously or exogenously. The post-translational modification is mainly catalyzed by poly (ADP-ribose) polymerase-1 (PARP-1) and hydrolyzed by poly (ADP-ribose) glycohydrolase (PARG). Numerous studies have demonstrated that PAR has a very short half-life (~1 min). It is promptly degraded by the 110-KDa PARG protein that is universally expressed in mammalian cells with both

KARGER

Fax +41 61 306 12 34
E-Mail karger@karger.ch
www.karger.com

1015-8987/12/0294-0361$38.00/0

Accessible online at:
www.karger.com/cpb

Ya-Lan Wang
Department of Pathology, Molecular Medicine & Cancer Research Centre
No. 1 Yixueyuan Rd, Chongqing, Med. University, Chongqing 400016 (China)
Tel. 0086-023-68485789, Fax 0086-023-68485111
E-Mail wangyalan074@126.com

endo-glycosidic and exo-glycosidic activity and cleaves PAR into free ADP-ribose units [1]. PARG is the main enzyme involved in this function and has a highly specific activity that maintains, in concert with PARP, intracellular PAR levels at low concentrations under homeostatic conditions [2-6].

Many studies have clarified the biological function of PAR and focused on the synthesis of the enzyme PARP. It has been demonstrated that PARP inhibitors, such as nicotinamide and 3-aminobenzamide, have beneficial effects on ischemia-reperfusion injury as well as in inflammation [7] both *in vivo* and *in vitro*. In addition, studies by Li and colleagues have documented that PARG inhibitors prevent cell death induced by hydrogen peroxide toxicity [8]. Since both PARG and PARP inhibitors decrease SAO (splanchnic artery occlusion) induced intestinal injury [9-11], PARG inhibition may be as effective as PARP inhibition for suppressing NAD/ATP depletion [12].

There are some data suggesting that PARP inhibitors could promote Akt activation during cardiac ischemia-reperfusion [13] and activated Akt in the presence of the PARP inhibitor could mediate the inhibition of MAP kinase, consequently preventing the activation of NF-κB and resulting in the consequent inhibition of inflammatory genes expression [14, 15].

Previously, we have demonstrated that the absence of PARP reduces the potencies of matrix adhesion, migration and invasion of colon carcinoma cells, and inhibits colon carcinoma liver metastasis in mice associated with decreasing NF-κB, MMP2 and MMP9 [16, 17]. Therefore, due to the dual relevance of both PARP and PARG in cancer progression, both the role and the mechanism of PARG in invasion and metastasis of colon carcinoma cells needs to be highlighted including its effect on metastasis related genes. Hence, experiments were performed both *in vitro* and *in vivo*, in order to determine whether silencing PARG could inhibit the metastatic behavior of colon carcinoma cells. These studies suggest the prospect for future introduction of PARG inhibitors in clinical trials.

Materials and Methods

In Vitro

Cell Culture. Human LoVo colon carcinoma cell line was grown and cultured in a 5% CO_2 incubator at 37°C in RPMI 1640 medium supplemented with 10% Fetal Bovine Serum (FBS), and, 100 U/ml of Penicillin and 100µg/ml of Streptomycin (Sigma-Aldrich).

To demonstrate that Akt phosphorylation could down-regulate metastatic related genes, 10µM of LY294002 (LY) which is an inhibitor of the PI3K/Akt pathway was used to treat PARG-shRNA transfected LoVo cells. Pyrrolidine dithiocarbamate (PDTC) a specific and selective inhibitor of NFκ-B was also used to show correlations between NF-κB, PARP and PARG.

LoVo Cell Transfection. Transfection was accomplished using lentiviral based short hairpin RNA (shRNA) vector (Sigma-Aldrich-TRCN00001265) with the following PARG-shRNA interference sequence:

CCG GGC GAT CTT AGG AAA CGG TAT TCT CGA GAG TAC CGT TTC CTA AGA TCG CTT TTT G, targeting PARG gene. For the control, non-target shRNA control transduction particles were used (Sigma-Aldrich). Transduction efficiency was optimized using pLKO.1 puro-TurboGFP (Sigma-Aldrich) as per the manufacturer's instructions.

LoVo cells were plated in a 96-well plate at 1.6×10^4 in each well, and cells were incubated until they reached 70% confluence. Next, media was gently aspirated, 200 µl of fresh RPMI-1640 was added together with 8 µg/ml Hexadimethrine bromide per well; 2, 5, 10 and 15 µl of lentivirus particles with TurboGFP were added, and the plate was left for incubation for 48 hours using triplicate wells. Fluorescence microscopy was used to assess the concentration of lentivirus that resulted in optimal transduction efficiency. It was found that the 10 µl lentiviral particle concentration displayed the maximum green fluorescent protein (TurboGFP) visible under microscopy (Fig. 1).

Subsequently, 10 µl of lentivirus particles of either non-target shRNA or PARG-shRNA were added to wells previously containing Hexamethrine bromide and were incubated for 48 hours. Media was then removed and 200µl of fresh media together with Puromycin to a final concentration of 8µg/ml (Sigma-Aldrich) was added to each well. Media was replaced with fresh media containing Puromycin every 2-3 days until resistant colonies could be identified.

Lastly, the experimental group consisted of LoVo cells transfected with PARG-shRNA (PARG-shRNA) while the controls included both untransfected LoVo cells (control) and LoVo cells transfected with non-targeting shRNA (control-shRNA). RT-PCR and Western Blot analysis were used to document PARG knockout in human LoVo colon carcinoma cells.

RT-PCR. Total RNAs was extracted from control, control-shRNA and PARG-shRNA LoVo cells with Trizol reagent (Takara) and reverse-transcribed to cDNA respectively. Genes were detected with a template of cDNA using the following oligonucleotide primers: PARG, 5'-CCA CCT CGT TTG TTT TCA-3' (sense) and 5'-CCA ACA TCT GGC AAA GGA-3' (antisense); PARP, 5'-CTA GAC AAC CTC CTG GAC ATCG-3' (sense) and 5'-CTC CCA GCA TTA TTA AGC CAAT-3' (antisense); NF-κB, 5'-GGG AAG GAA CGC TGT CAG AG-3' (sense) and 5'-TAG CCT CAG GGT ACT CCA TCA-3'(antisense); β-Actin, 5'-GTC AAG AAA GGG TGT AAC GCA AC-3' (sense) and 5'-TCC TGT GGC ATC CAC GAA ACT-3' (antisense). Thirty-five PCR cycles were used for the amplification of reverse transcriptase products (94°C for 30 s, 50~58°C for 30 s, 72°C for 1 min and then 5 min for the last

extension). PCR amplification products were separated on a 1.8% agarose gel. This experiment was performed in triplicate.

Western Blot Analysis. Cells were washed once with phosphate buffered saline (PBS) and collected by scraping into individual EP tubes. Proteins were extracted according to protein extraction protocols and protein concentrations determined using the Coomassie Blue assay (Pierce Biothechnology). Protein extracts (20µg/lane) were loaded and electrophoresed using 10% polyacrylamide gels (SDS-PAGE) followed by transfer to PVDF membranes (Millipore) and blocking with 5% non-fat dry milk for 2h. Primary antibodies against PARG (Abcam), PARP, NF-κB, MMP2, MMP9, Akt, Phospho-Akt Serine^{473}(Santa Cruz Biotechnology) were incubated overnight at 4°C. Secondary antibodies (peroxidase-conjugated goat or anti-rabbit IgG) were incubated for 1h at 37°C. Blots were washed three times, exposed to chemiluminescence reagents (Pierce Biotechnology), exposed to photographic film (Bio-Rad) and evaluated by densitometric analysis using Quantity One software [18]. All experiments were performed in triplicate.

Nuclear Protein Extraction Preparation. Nuclear protein extracts were prepared from cells grown to 90% confluence and performed on ice with ice-cold reagents. Cells 5 x 10^6 were scraped into 1ml PBS, washed twice, supernatant was discarded and the pellet was suspended into 500 µl Hypotonic Buffer and incubated on ice for 15 minutes. 25 µl of 10% Nonidet P_40 was added, cells were vortexed for 10 seconds and after which, centrifuged for 10 minutes at 3000 rpm at 4°C. The supernatant containing the cytoplasmic fraction was discarded and the pellet containing only the nuclear fraction was resuspended into 50µl complete Cell Extraction Buffer for 30 minutes on ice with occasional light vortexing. Nuclear extracts were recovered after centrifugation for 30 minutes at 14,000 g x 4 at 4°C. Protein concentrations were determined using Coomassie Blue assay reagent (Pierce Biotechnology).

Electrophoretic Mobility Shift Assay (EMSA). LightShift® Chemiluminescent EMSA Kit (Pierce Biotechnology) was used to determine NFκ-B activation as per manufacturer's protocol. A native polyacrylamide 4% gel was prepared that was pre-electrophoresed at 100V for 40 min. NF-κB was labeled with Biotin-labelled oligonucleotides (5'-AGT TGA GGG GAC TTT CCC AGG C-3') and each sample (20µg/ml) was loaded onto the gel and run again at 100V until the stain had migrated through ¾ of the gel. Next, nuclear extractions were transferred to nylon membranes (Sigma-Aldrich) and DNA crosslinked to the membranes using a commercial UV light activated cross-linker. The membrane was treated with blocking buffer for 15 min, washed and reincubated with conjugate/blocking buffer for 15 min. Afterwards, membrane was washed 4 times and transferred to substrate equilibration buffer for 5 min, and lastly to substrate working solution for 5 min. The membrane was blotted and exposed to X-ray film for 2 min. The experiment was repeated in triplicate.

Cell Migration and Invasion Assays. The cell migration assay used 8.0µm pore size Transwell inserts (Costar Corp) as described formerly with some modification [10]. The under surface of the membrane was coated with fibronectin (FN-10µg/ml) (Sigma Chemical Co) in PBS for 2 hours at 37°C. The lower chamber was filled with 500µL of RPMI 1640 medium with 10% fetal bovine serum (FBS). LoVo cells were resuspended into the migration medium (serum-free RPMI1640) and 1x10^5 cells in 200µL of medium were added to the upper chamber after being washed twice with PBS. After 24 hours of incubation at 37°C, the cells on the upper surface of the membrane were gently and carefully scraped out using cotton tips. The migrant cells that were adherent to the lower surface of the membrane were fixed in 10% formalin at room temperature for 10 min, and then stained with H&E (Hematoxylin and Eosin stain). The results of the cell migration assay were evaluated by counting the number of cells on the lower surface of the membrane under an inverted microscope in five different fields at a magnification of x400. Whereas, for the cell invasion assay, the only difference was that the cells (1x10^5 in 200µL of 1640 with serum-free) were seeded onto Geltrex™ (Invitrogen) coated to the upper chamber according to the manufacturer's instructions. Cells that had crossed the Geltrex™ and passed through the pores of the filter were counted in five fields at x400 [19]. The results are representative of three different experiments.

Cell Adhesion Assay. LoVo cell adhesion assay was accomplished as described by Arai et al [20]. Flat bottom culture plates with 96 well formats were overlayed with 40µl of FN (10µg/ml) in PBS overnight at 4°C; then blocked with 0.2% bovine serum albumin (BSA) for 2 hours at room temperature followed by washing twice with RPMI 1640; the cells were resuspended in media and seeded at 4x10^4cells/well (200µL) in triplicate and incubated for 2 hours at 37°C. In order to remove any unbounded cells, plates were washed three times with medium. Cells remaining attached to the plates were counted using 3-(4 5-dimethyl-2-thiazolyl)-2,5-diphenyl-^{2}H-tetrazolium bromide (MTT) assay. 50µl per well of MTT solution (2mg/ml diluted in PBS-Sigma Aldrich) was added, plates were incubated for 4 hours at 37°C and finally, 150µl of dimethyl sulfoxide (DMSO) was added after discarding the supernatant. The absorbance (OD) was read via a universal plate reader (Bio-Tek) at 630 nm. The percentage of adherent LoVo cells was estimated by (OD of control group- OD of experimental group)/OD of control group x100%. This experiment was done at least three times per condition tested.

In Vivo

Establishment of Animal Model of Liver Metastasis of Colon Carcinoma. 18 Balb/c female mice, 6-8 weeks old, weighing 18-21g were supplied by the animal laboratories of Chongqing Medical University, China and the animal experiments were conducted and approved in accordance with our institutional guidelines and ethics committee. CT26 (mouse derived colonic carcinoma cell line) cells were cultured and successfully transfected similarly to LoVo cell transfection (materials and methods), where untransfected, control-shRNA and PARG-shRNA groups were grown according to similar conditions of cell culture and the cell number was adjusted to a final concentration of 1 x 10^7cells/ml [17]. Mice were anaesthesised intraperitoneally with 2% chloral hydrate (15ml/kg) and cancer cells 5 x 10^5 in 0.05 ml PBS was injected under splenic capsule of each mouse. All mice had free access to food and water throughout the experiment. On day 14, all mice

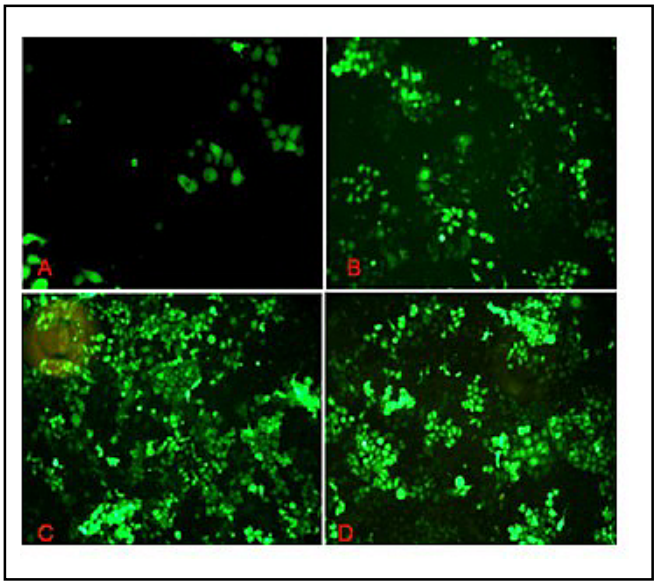

Fig. 1. LoVo cells transfected with TurboGFP (x400). 2 (A), 5 (B), 10 (C) and15μL (D) of lentiviral particles containing TurboGFP were transfected into LoVo cells. After 48h of incubation at 37°C, fluorescin was displayed in LoVo cells.

were sacrificed and the size and number of metastatic nodules in the liver were examined upon sectioning of the liver. Individual tumor volumes (V) were estimated as $V=ab^2/2$; where a is the maximum diameter and b is the minimum diameter. The total volume was recorded if there were more than 2 metastatic nodules. Grossly evident liver metastatic nodules was quantitated and graded as grade 0: no liver metastasis; grade I: 1-5 liver metastatic nodules; grade II: 6-50 liver metastatic nodules; and grade III: more than 50 liver metastatic nodules and mass fusion making it difficult to assess, according to previous classification [17].

Statistical Analysis

Statistical analysis was performed by one-way ANOVA or Student's t test using SPSS 11.5 software package. A P value less than 0.05 ($P<0.05$) was set as the criterion for statistical significance.

Results

Knockdown of PARG expression by transfection with shRNA lentivirus in LoVo cells

To verify the efficacy of PARG inhibition by lentiviral shRNA, RT-PCR and western blot analysis were performed following transfection and revealed that PARG was almost completely absent in treated LoVo cells (PARG-shRNA) compared with both control groups. As expected PARG expression was not affected by an empty vector transfection (Fig. 2a-d).

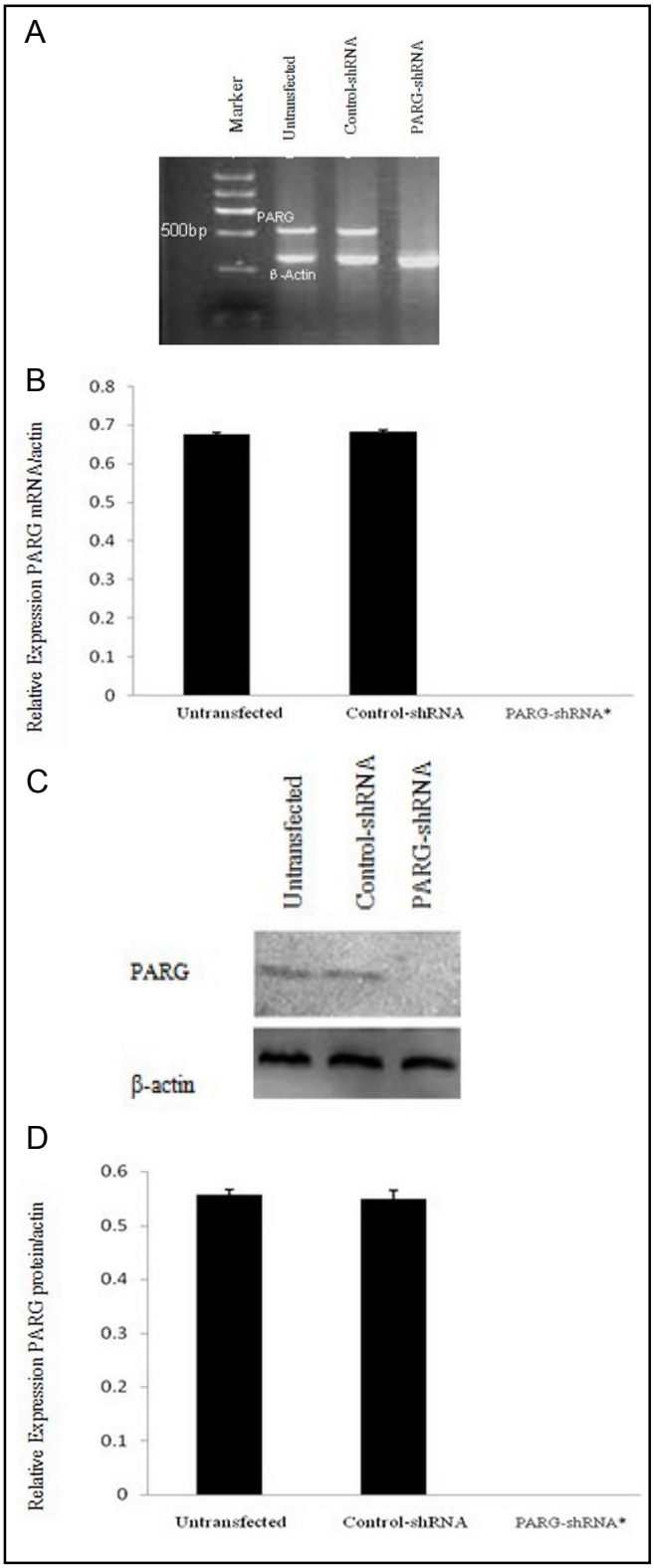

Fig. 2. Effect of PARG knockdown by shRNA in LoVo cells. RT-PCR (a & b) and western blot (c & d) analyses reveals complete inhibition of PARG mRNA and protein expression in PARG-shRNA transfected cells compared to untransfected and control-shRNA cells. β-actin was used as an internal loading control.

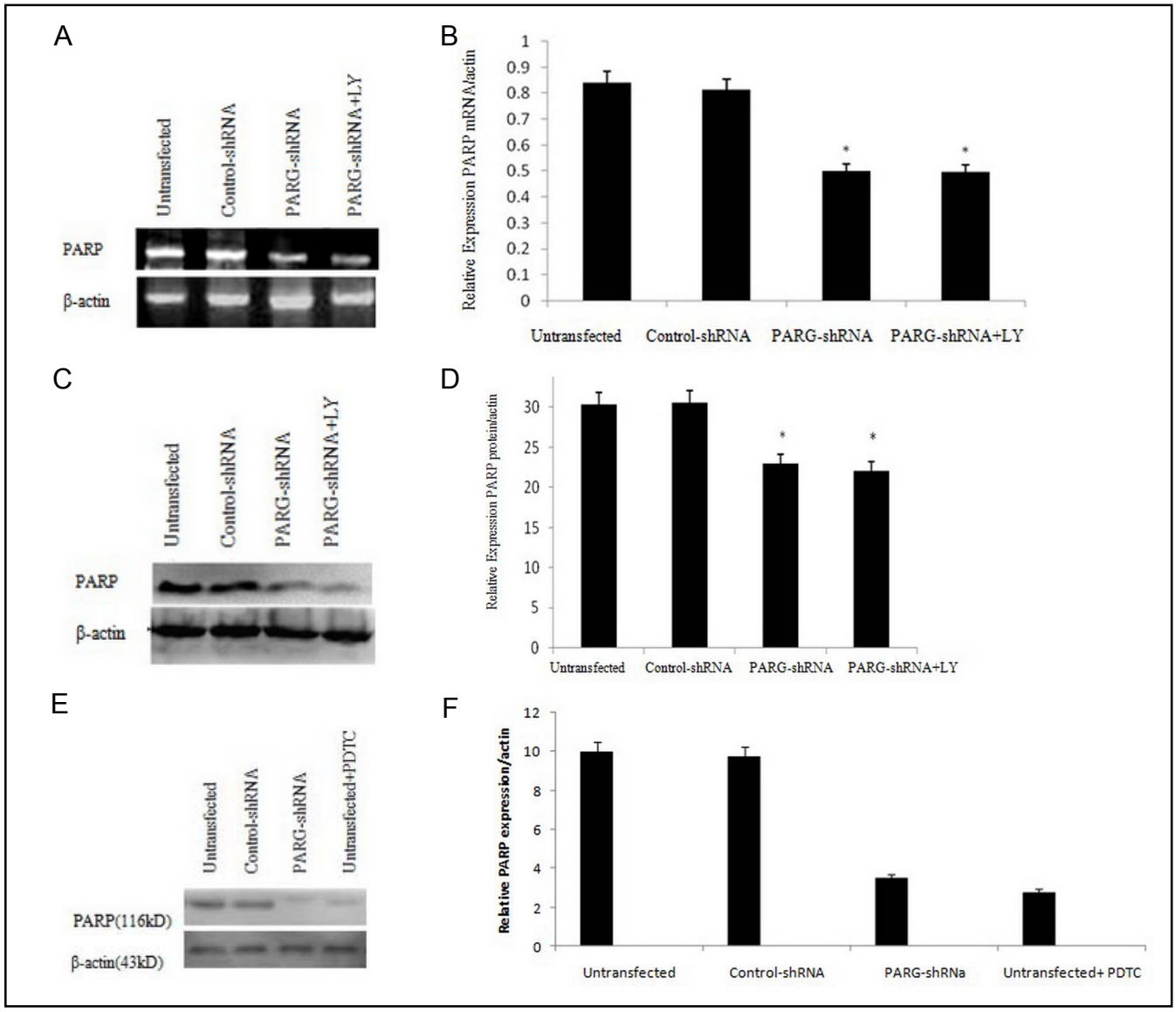

Fig. 3. PARG suppression affects PARP expression. Both RT-PCR (a & b) & western blotting (c & d) show that PARG deficient cells display a decreased expression of PARP mRNA and protein ($P^*<0.05$) compared to both controls. However, no further obvious change was noted in expression of PARP in PARG-shRNA+LY treated cells compared with PARG-shRNA LoVo cells. β-actin was used as loading control. PDTC (pyrrolidine dithiocarbamate), an NF-κB selective inhibitor, decreases PARP expression in human LoVo cell compared to untransfected and control-shRNA cancer cells (e & f). PARG-shRNA transfected cells also show a similar decrease in PARP expression ($P^*<0.05$) compared to both controls.

PARG attenuation affects PARP expression and pyrrolidine dithiocarbamate (PDTC) effectively suppresses PARP expression

PARP and PARG are enzymes that modify target proteins by the addition and removal of ADP-ribose polymers. Some researchers have reported that these two nuclear enzymes with opposing enzymatic activities act in a similar, rather than in an antagonistic manner to regulate gene expression in some pathological conditions. So, in this study, we also detected the impact of PARG suppression on PARP where interestingly, we found that PARP expression was inhibited in PARG-shRNA confirmed by mRNAand protein levels which was not observed in untransfected or the control shRNA group (Fig. 3a-d).Hence, in our previous experiments, we found that 5-Amimoisoquinolin-1-one (5-AIQ) which is an inhibitor of the catalytic activity of PARP could inhibit the activity of the latter as well as its expression and decrease NF-κB; therefore at that time we speculated that NF-κB could be involved in the synthesis of PARP

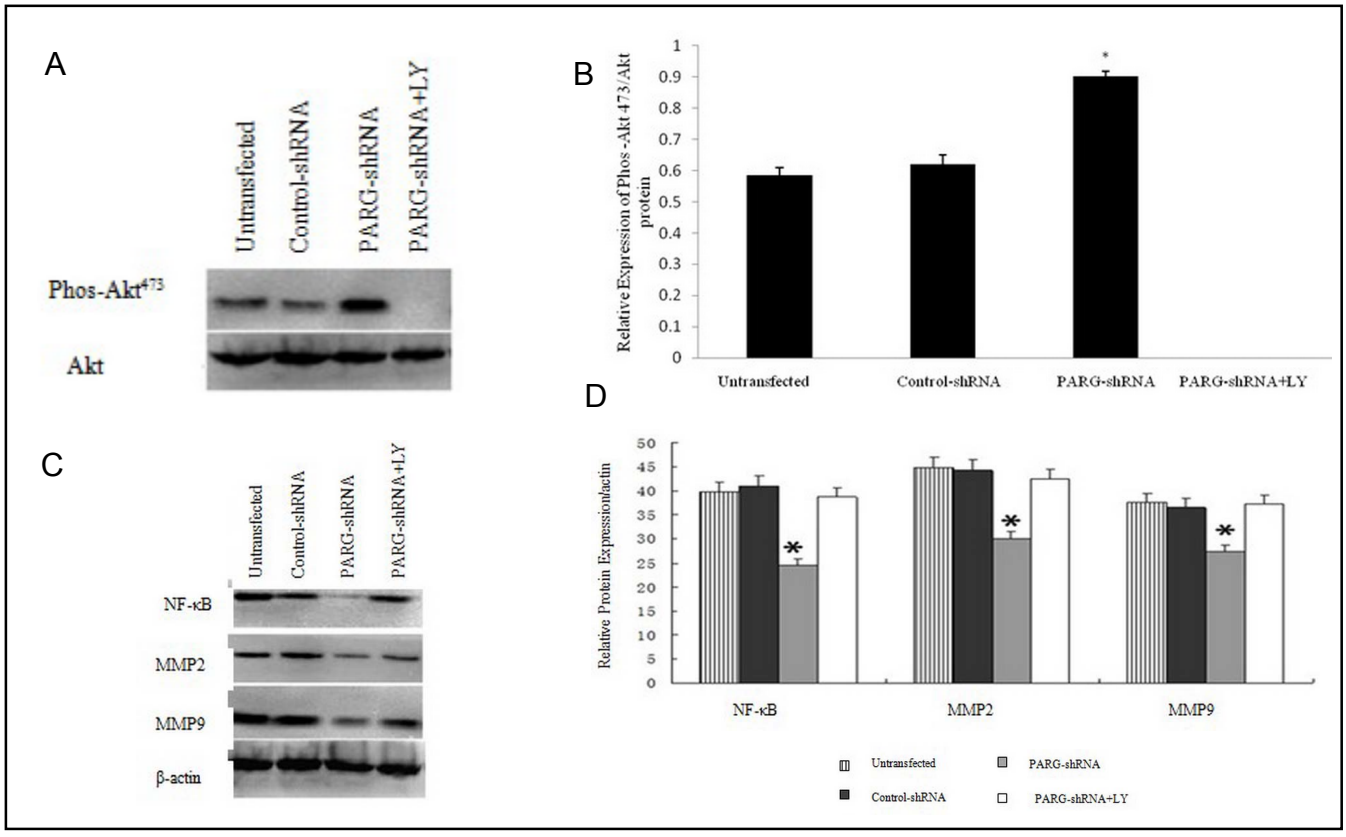

Fig. 4. PARG inhibition increases Akt phosphorylation. Densitometric analysis of phosphorylated Akt band intensity normalized with the intensity of Akt the data are represented as mean±SD of independent experiments performed in four different experiments; where $P^*<0.05$ compared with untransfected and control-shRNA cells (a & b). Besides, complete inhibition of phosphorylated Akt in PARG-shRNA+LY cells was noted showing effectiveness of LY294002 inhibitor. Effect of PARG deficiency on NF-κB, MMP2 and MMP9 expressions. In PARG-shRNA transfected cells there was a decrease of NF-κB, MMP2 and MMP9 band intensities ($P^*<0.05$) in comparison to controls. Data are expressed as means±SD of four different experiments (c & d).

[21]. PDTC, a selective NF-κB inhibitor was used to prove this speculation. The results showed that untransfected LoVo cells treated with PDTC showed a decrease in the PARP expression compared to untransfected without PDTC and control-shRNA cells ($P^*<0.05$); nevertheless showing similar result to PARG-shRNA transfected cells. Therefore, underlining the close relationship between PARG, PARP and NF-κB (Fig. 3e, f).Moreover, no further change of PARP expression was noted in PARG-shRNA+LY treated cells compared with PARG-shRNA LoVo cells (Fig. 3a-d), therefore showing that the LY inhibitor on PARG-shRNA cells does not affect PARP.

Silencing PARG activates PI3K/Akt pathway and downregulates its downstream targets

Given the biological importance of the PI3K/Akt pathway in cancer progression and metastasis, we investigated the effect of PARG suppression on this pathway by determining the level of Akt phosphorylation. Western blot revealed that (Fig. 4a, b) the expression of phospho-Akt^{473} in LoVo cells was much higher in the PARG-shRNA group than in both control groups indicating that PARG knockdown activated PI3K/Akt signal pathway.

We then examined potential downstream targets of the PI3K/Akt pathway in LoVo cells after PARG knockdown. Western blot results (Fig. 4c, d) showed reduced expression of NF-κB, MMP2 and MMP9 in PARG-shRNA group than in both control groups. This indicates that PARG suppression decreases the protein levels of these metastasis related factors while similarly to our assumption, expression of NF-κB, MMP2 and MMP9 were unaltered by treatment with LY in PARG-deficient LoVo cells, compared with the control groups. This demonstrates that PARG suppression decreases NF-κB, MMP2 and MMP9 expressions via activation of PI3K/Akt pathway in LoVo cells (Fig. 4c, d).

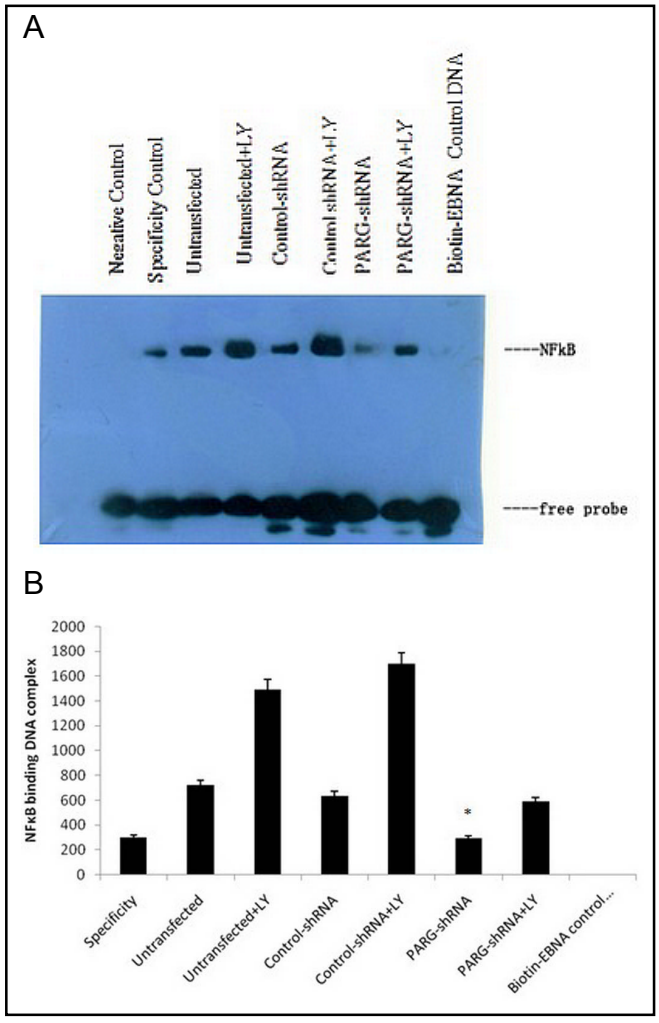

Fig. 5. The Effect of PARG inhibition on binding of NF-κB to DNA in LoVo cell line. Electrophoretic mobility shift assay was performed with nuclear extracts of respective LoVo cells-untransfected and control-shRNA with and without LY, and PARG-shRNA with and without LY (a). The negative control consisting of reaction buffer only had no visible NF-κB band. The band intensity was much higher in both untransfected+LY and control-shRNA+LY compared with PARG-shRNA where there was a large reduction in intensity of the band (P*<0.05) (b). The results shown represent three independent experiments.

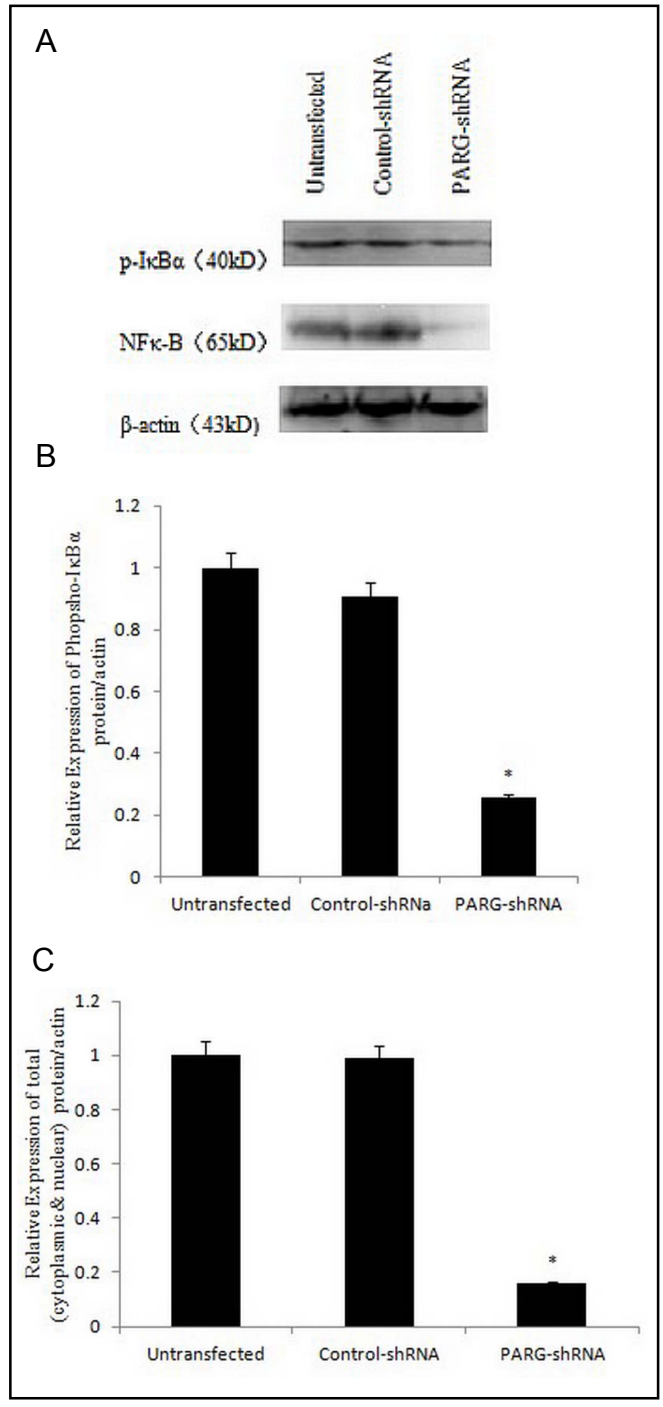

Fig. 6. (a-c)**.** Western blot analysis highlights a decrease in expression of cytoplasmic phosphorylated IκBα together with a fall in the intranuclear expression of NF-κB in PARG-shRNA cells compared to both untransfected and control-shRNA cells (P*<0.05).

Effect of PARG inhibition on Binding of NF-κB to DNA

No NF-κB band was visible in the negative control consisting of reaction buffer while the band intensity was much higher in both untransfected+LY and control-shRNA +LY compared with PARG-shRNA where there was a large reduction in NF-κB levels by western blot (P*<0.05) (Fig. 5a, b). This confirmed our western blot result where suppression of the PI3K/Akt pathway was associated with increased NF-κB binding to DNA complex. Treatment with both PARG-shRNA+LY did not have any effect on binding NF-κB compared with both controls.

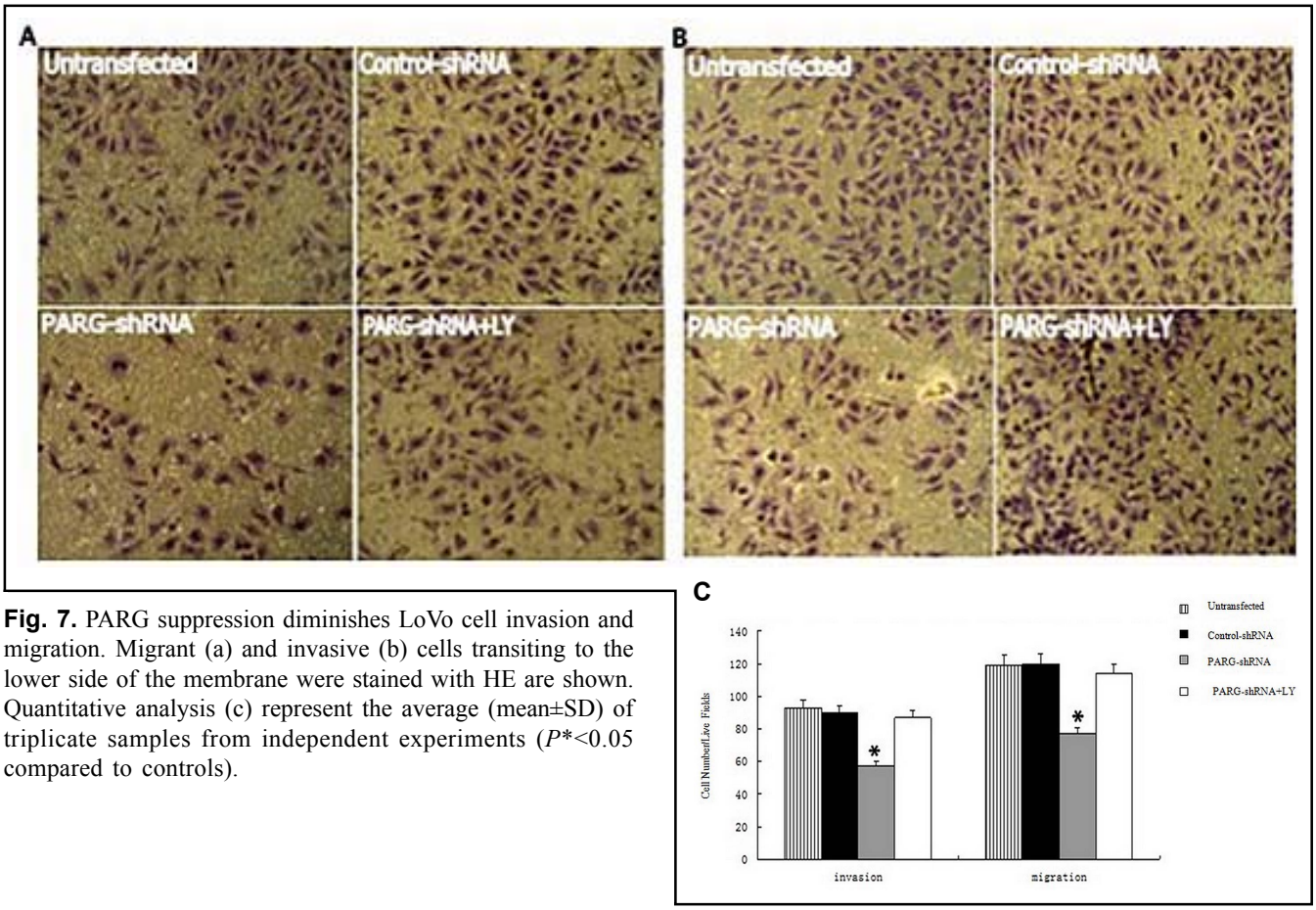

Fig. 7. PARG suppression diminishes LoVo cell invasion and migration. Migrant (a) and invasive (b) cells transiting to the lower side of the membrane were stained with HE are shown. Quantitative analysis (c) represent the average (mean±SD) of triplicate samples from independent experiments (P*<0.05 compared to controls).

Groups	Value	Inhibition ratio (%)
Untransfected	0.0781±0.0010	-
Control shRNA	0.0775±0.0010	0.7682
PARG-shRNA	0.0584±0.0012	25.22*
PARG-shRNA+LY	0.0773±0.0012	1.024

Table 1. Effect of PARG suppression on LoVo cell adhesion to fibronectin matrix protein by MTT, ($\bar{x}\pm s$, $n=3$). Data are mean±SEM. *P<0.05 versus untransfected or control-shRNA groups.

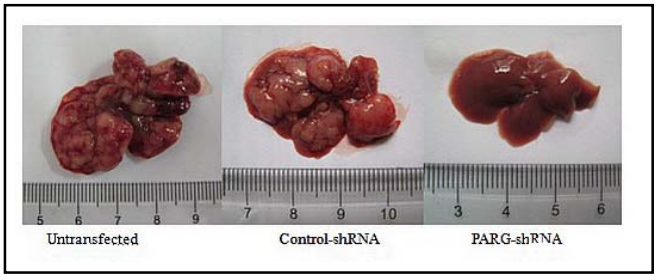

Fig. 8. Mouse model of liver metastasis in colon cancer. Both untransfected and control-shRNA CT26 groups displayed more liver metastatic nodules compared to the PARG-shRNA group (P<0.05).

Intranuclear expression of NF-κB in PARG-shRNA Lovo cells

Western Blot analysis of the cytoplamic extraction fraction showed that in different nomenclature PARG-shRNA treated cells, expression of phosphorylated IκBα (p-IκBα) was decreased as well as the relative intranuclear protein expression of NF-κB. This suggested that in cells where PARG was silenced there was a decrease in intracytoplasmic expression of phosphorylated IκBα resulting in an intranuclear decrease of NF-κB (Fig. 6a-c).

Suppression of PARG weakens in vitro migratory, invasive and adhesive properties of human LoVo colonic cancer cells via the PI3K/Akt pathway

We investigated whether PARG suppression could affect the malignant biological properties of LoVo cells *in vitro*, in particular migration, invasion and adhesion.

Group	n	The grading of liver metastatic tumor nodules			
		0	I	II	III
Untransfected mice	6	0	0	2	4
Mice transfected with empty vector: Control-shRNA	6	0	0	3	3[a]
Mice transfected with shRNA lentivirus targeting PARG: PARG-shRNA	6	5	0	1	0[bc]

Table 2a. Comparison of metastatic tumor nodules in the liver of mice in untransfected, control-shRNA and PARG-shRNA groups. a. $P>0.05$,control-shRNA vs untransfected b. $P<0.05$,PARG-shRNA vs untransfected c. $P<0.05$,PARG-shRNA vs control-shRNA. PS: Statistical analysis is combined with Kruskal-Wallis and Nemenyi methods. Liver metastasis nodules grading: 0 level: no naked eye metastatic nodules: I level: 1-5 metastatic nodules; II level: 6-50 metastatic nodules; III level: more than 50 metastatic nodules or mass fusion making it difficult to count.

Group	Weight/mg	Volume *(V)*/cm3
Untransfected	1098.33±277.93	1.17±0.46
Control-shRNA	1092.83±165.71[a]	1.18±0.30[a]
PARG-shRNA	293.33±126.12[bc]	0.26±0.13[bc]

Table 2b. Individual tumor volumes (*V*) were estimated as $V=ab^2/2$, where *a* is the maximum diameter and *b* is the minimum diameter. a. $P>0.05$,control-shRNA vs untransfected b. $P<0.05$,PARG-shRNA vs untransfected c. $P<0.05$,PARG-shRNA vs control-shRNA. Statistical analysis was performed using One-way ANOVA to specify its significance.

First, cells were cultured for 24h and those having migrated onto the other side of the pored filters were counted under the microscope. As shown in Fig. 7A, C, the PARG-shRNA cells exhibited significant decrease in cell number as compared to both untransfected and control-shRNA cells ($P^*<0.05$, $P^*<0.05$). The invasive ability of cells was evaluated using invasion chambers *in vitro* where PARG deficient cells exhibited a remarkable decrease in invasiveness in comparison to the respective controls (Fig. 7B, C). When treated with LY, no important change was noted compared to both controls.

Cell adhesion is a prerequisite for cell migration and thus we next investigated whether PARG suppression could affect cell adhesion to extracellular matrix substrates such as fibronectin. PARG-deficient LoVo cells showed a significantly decreased adhesion to fibronectin compared with control groups. As expected, the PARG-shRNA cells treated with LY has no significant change in relation to cell adhesion (Table 1). In sum, these results demonstrate that PARG silencing suppressed migratory, invasive and adhesive abilities of LoVo cells likely mediated by the activation of PI3K/Akt pathway.

In Vivo Metastasis Model Observation

On day 14 following injection of LoVo cells, the mice were sacrificed, abdominal laparotomy was performed and liver metastatic nodules were counted. Both controls had grade II-III liver metastasis (Fig. 8) compared to PARG-shRNA group ($P<0.05$) where 5 mice had no liver metastatic nodules and only one had grade II metastasis (Fig. 8, Table 2a). Moreover, the volume *(V)* of tumor mass in cm^3 (Fig. 8, Table 2b) was lower in PARG-shRNA compared to untransfected and control-shRNA groups ($P<0.05$). Thus PARG suppression does appear to play a critical role in the prevention of cancer dissemination and metastasis *in vivo*.

Discussion

In our current study, we have provided the initial insights into the probable mechanism by which PARG deficient LoVo cells displayed a decrease in both invasion and metastasis. It has been known that both PARG and PARP do play important roles in reticular biological

processes [12] where PARP deficiency could reduce arthritis severity in an animal experimental model [22] and diminish tumor necrosis factor-induced inflammatory damage in rheumatoid synovial fibroblasts [23] while, PARG inhibition could prevent septic shock-like syndrome [10] and decrease spinal cord inflammation [24]. Furthermore, some studies have highlighted similar effects on many biological endpoints between PARP and PARG [9-11] and their functional similarities [12, 25-26] have been accepted as well. In other specific pathophysiological processes, their relationship is more agonistic [12, 25]. In some experimental systems, PARP suppression has been shown to attenuate transcription factor activation and inflammatory responses mediated via activation of PI3K/Akt pathway [14]; this correlates with our findings of PARG deficiency resulting in activation of this pathway in LoVo cells.

Our study shows the relevance and effectiveness of silencing PARG expression in the field of colon carcinoma migration and invasion *in vitro* and metastasis *in vivo* via PI3K/Akt pathway, a cascade known to be pivotal in cancer pathogenesis, progression and metastasis [27]. The LoVo cell line was successfully transfected by a specific lentivirus vector-mediated short hairpin RNA in PARG-shRNA cells that completely inhibited PARG expression (Fig. 1a-d). Our experiments compared 4 major groups, namely untransfected, control-shRNA, PARG-shRNA and PARG-shRNA+LY which were assessed for a decrease in PARP. PARP suppression was clearly noted in PARG-shRNA cells (Fig. 3a-d) and the result was consistent with our previous work [28]. In addition, recent studies have shown that PARP inhibition decreases NF-κB expression which is important in cancer proliferation and metastasis [21, 29-30]. We had previously demonstrated that 5-Amimoisoquinolin-1-one (5-AIQ), an inhibitor of the catalytic activity of PARP, could inhibit PARP activity as well as its expression was associated with decrease in NF-κB [21]. At that time we hypothesized that NF-κB could be involved in the synthesis of PARP; in this present experimental study we have confirmed the relationship between them. We used pyrrolidine dithiocarbamate (PDTC), a specific NF-κB inhibitor in untransfected cells to emphasize that PARP expression is suppressed with inhibition of NF-κB (Fig. 3e, f). This highlighted the interactions between PARG, PARP and NF-κB [21, 28, 29]. PARG-shRNA LoVo cells showed increased phosphorylation of Akt with an attenuation of the total NF-κB expression (Fig. 4a-d) which is also supported by these studies using either a PARP or PARG inhibitor [13, 14, 18, 31]. Yet, until now there was no concrete evidence regarding a similar role for PARG inhibition on Akt activity. Our experiments enlighten some aspects of PARG suppression in relation to hinderance cancer progression. LY294002, an effective inhibitor of PI3K/Akt pathway [26, 32], was used to probe the relationship between PARP, PARG, PI3K/Akt pathway, NF-κB and downstream genes such as MMP2 and MMP9. EMSA results confirmed that inhibition of PARG decreases the amount of the nuclear NF-κB–DNA binding complex in LoVo cells compared to both controls (Fig. 5a, b). Suppression of the PI3K/Akt pathway in untransfected+LY and control-shRNA+LY resulted in increased levels of NF-κB–DNA binding complex. Together these results indicate that PARG deficiency results in upregulation of phosphorylated Akt and a decrease in NF-κB expression (Fig. 4a-d) and suppression of the PI3K/Akt pathway results in a surge in NF-κB levels (Fig. 5a, b). This emphasizes the relationship of PARG silencing with PI3K/Akt/NF-κB pathway. Previously we reported that PARP inhibition decreased metastatic potency of mouse colorectal carcinoma CT26 cells *in vivo* and *in vitro* via suppressing the expressions of metastasis related genes NF-κB, MMP2 and MMP9 [16, 17]. Similarly, it was found that PARG knockout cells displayed a decrease in NF-κB, MMP2 and MMP9 expressions with an increase in band intensity in phosphorylated Akt. However, PARG-shRNA+LY cells did not result in further assayed effects as compared to untransfected and control-shRNA cells (Fig. 4c, d). This suggests that PARG inhibition may be a fruitful way to inhibit LoVo cell matrix adhesion, invasion and migration and related protein expression important in colon carcinoma, one of the commonest cancers in the world with low survival rates when no longer amenable to surgical intervention. Likely, PARG and PARP suppression cooperate to downregulate NF-κB and its metastasis related genes MMP2 and MMP9 through the upstream regulation of PI3K/Akt pathway. Moreover, it is known that Akt activates IKK kinases such that upon phosphorylation, IκBα is degraded and thus enabling NF-κB to undergo nuclear translocation. This classical pathway is considered to be the mode of activation of NF-κB assessed by intranuclear p65 dimer [33, 34]. We have confirmed that in PARG-shRNA cells, cytoplasmic expression of phosphorylated IκBα expression is reduced leading to a simultaneous fall in intranuclear NF-κB p65 subunit (Fig. 6a-c) together with its total protein expression (Fig. 3c, d). This demonstrates diminished activation of NF-κB in PARG-shRNA cells resulting in decreased expression of its dependent genes [35-38] including

MMP2 and MMP9 (Fig. 4c, d). Further functional *in vitro* studies showed that PARG-shRNA transfected cells manifest reduced cell invasion, migration and adhesion abilities (Fig. 7A-C, Table 1). It has been known for over 10 years that inhibition of PARG leads to inhibitory automodification of PARP-1 [11]. Thus in our experiment it is probable that PARG knockdown led to PARP inhibition [11, 23] which in turn resulted in activation of PI3K/Akt pathway. Alternatively, it could be PARG suppression could directly activate the PI3K/Akt pathway. Previously we reported that PARP inhibition in CT26 cells also suppressed NF-κB along with its related metastatic genes [16, 17] and now similar effects are noted in our current experiment. Perhaps PARG and PARP work together and are directly correlated to each other or maybe it is only the action of PARG that has led to our outcomes; additional studies are needed to explore these options.

In vivo studies were conducted with the objective of enhancing and supporting our *in vitro* experiments as in our previous studies [16, 17], where CT26 cells were transfected under similar conditions as LoVo cells and our results demonstrated that transfection of PARG-shRNA CT26 cells could inhibit effectively the metastasis of of colon carcinoma cells implanted in mouse spleen. The number of liver metastatic nodules according to our staging (Fig. 8, Table 2a) was significantly lower in the PARG-shRNA group ($P^*<0.05$) compared to both untransfected and control-shRNA groups and the tumor volume was smaller in comparison to both control groups (Fig. 8, Table 2b). This indicates that deficiency of PARG could inhibit the metastasis behavior of colon carcinoma in our model.

In brief, our results imply that PARG and PARP inhibition led to the suppression of NF-κB and its downstream targets MMP2 and MMP9 and the upregulation of PI3K/Akt pathway which was demonstrated to be important for cell proliferation, invasion and metastasis in LoVo cell line [26, 39]. Moreover, this fact is strengthened by our *in vivo* results showing that PARG could play an important role in reducing the metastatic potential of colon carcinoma to the liver in our model. PARG suppression in relation to elevated PI3K/Akt is an important mechanism in our colon cancer model, but clearly not an exclusive and ultimate treatment for colon carcinoma or its metastases. Since PARP inhibitors have been introduced in clinical trials for quite some time now and that both PARP and PARG inhibition acted in a similar manner in colon carcinoma, our findings on PARG may provide a new target for clinical colon cancer therapy. Despite this apparent promise, more work is needed to determine whether effective PARG inhibitors should be introduced in clinical trials for the benefit of cancer patients.

Acknowledgements

This work was supported by the National Nature Science Foundation of China (NSFC: 30870946). Moreover, we would like to thank Lin Xiao, Yang Chun-rong, Bu You-quan for their excellent technical help.

References

1 Davidovich L, Vodenicharov M, Affar EB, Poirier GG: Importance of Poly(ADP-ribose) glycohydrolase in the control of poly(ADP-ribose) metabolism. Exp Cell Res 2001;268:7-13.

2 de Murcia G, de Murcia JM: Poly(ADP-ribose) polymerase: a molecular nick-sensor. Trends Biochem Sci 1994;19:172-176.

3 Shall S, de Murcia G: Poly(ADP-ribose) polymerase-1: what have we learned from the deficient mouse model? Mutat Res 2000;460:1-15.

4 Hong SJ, Dawson TM, Dawson VL: Nuclear and mitochondrial conversations in cell death: PARP-1 and AIF signaling.Trends Pharmacol Sci 2004;25:259-264.

5 Jagtap P, Szabo C: Poly(ADP-ribose) polymerase and the therapeutic effects of its inhibitors. Nat Rev Drug Discov 2005;4:421-440.

6 Schreiber V, Dantzer F, Ame JC, de Murcia G: Poly(ADP-ribose): novel functions for an old molecule. Nat Rev Mol Cell Biol 2006;4:517-528.

7 Cuzzocrea S, Riley DP, Caputi AP, Salvemini D: Antioxidant therapy: a new pharmacological approach in shock, inflammation, and ischemia/reperfusion injury. Pharmacol Rev 2001;53:135-159.

8 Li J, Zhang J: Pharmaceutical compositions containing poly(ADP-ribose) glycohydrolase inhibitors for inhibiting or decreasing free radical-induced cellular energy depletion, cell damage or cell death. WO 2000;00025787.

9 Di Paola R, Genovese T, Caputi AP, Threadgill M, Thiemermann C, Cuzzocrea S: Beneficial effects of 5-aminoisoquinolinone, a novel, potent, water-soluble, inhibitor of poly (ADP-ribose) polymerase, in a rat model of splanchnic artery occlusion and reperfusion. Eur J Pharmacol 2004;492:203-210.

10 Genovese T, Di Paola R, Catalano P, Li JH, Xu W, Massuda E, Caputi AP, Zhang J, Cuzzocrea S: Treatment with a novel poly(ADP- ribose) glycohydrolase inhibitor reduces development of septic shock-like syndrome induced by zymosan in mice. Crit Care Med 2004;32:1365-1374.

11 Virag L, Szabo C: The therapeutic potential of poly (ADP-ribose) polimerase inhibitors. Pharmacol Rev 2003;54:375-429.
12 Cuzzocrea S, Di Paola R, Mazzon E, Cortes U, Genovese T, Muià C, Li W, Xu W, Li JH, Zhang J, Wang ZQ: PARG activity mediates intestinal injury induced by splanchnic artery occlusion and reperfusion. FASEB J 2005;19:558-566.
13 Pálfi A, Tóth A, Kulcsár G, Hantó K, Deres P, Bartha E, Halmosi R, Szabados E, Czopf L, Kálai T, Hideg K, Sümegi B, Tóth K: The role of Akt and Mitogen-Activated Protein Kinase Systems in the Protective Effect of Poly(ADP-Ribose) Polymerase Inhibition in Langendorff Perfused and in Isoproterenol-Damaged Rat Hearts. J Pharmacol Exp Ther 2005;315:273-282.
14 Veres B, Radnai B, Gallyas F Jr, Varbiro G, Berente Z, Osz E, Sumegi B: Regulation of Kinase Cascades and Transcripition Factors by a Poly(ADP-Ribose) Polymerase-1 Inhibitor, 4-Hydroxyquinazoline, in Lipopolysaccharide-Induced Inflammation in Mice. J Pharmacol Exp Ther 2004;310:247-255.
15 Guha M, Mackman N: The phosphatidylinositol 3-kinase-Akt pathway limits LPS activation of signaling pathways and expressing of inflammatory mediators in human monocytic cells. J Biol Chem 2002;277:32124-32132.
16 Li M, Wang Y: Effect of PARP inhibition on invasiveness of mouse colon carcinoma cell line. J Sun Yat-Sen Univ (Med Sci) 2008;29:388-392.
17 Qin Y, Wang Y, Li Y: Effect of Poly(ADP-ribose)polymerase inhibition on liver metastasis of mouse colorectal carcinoma CT26 cell line in vivo. J Fourth Mil Med Univ 2008;29:1621-1624.
18 Erdèlyi K, Kiss A, Bakondi E, Bai P, Szabó C, Gergely P, Erdödi F, Virag L: Gallotannin Inhibits the Expression of Chemokines and Inflammatory Cytokines in A549 Cells. Mol Pharmacol 2005;68:895-904.
19 Wu X, Zeng H, Zhang X, Zhao Y, Sha H, Ge X, Zhang M, Gao X, Xu Q: Phosphatase of Regenerating Liver-3 Promotes Motility and Metastasis of Mouse Melanoma Cells. Am J Pathol 2004;164:2039-2054.
20 Arai A, Nosaka Y, Kohsaka H, Miyasaka N, Miura O: CrkL activates integrin-mediated hematopoietic cell adhesion through the guanine nucleotide exchange factor C3G. Blood 1999;93:3713-3722.
21 Li Cai, Threadgill MD, Wang YL, Ming Li: Effect of Poly (ADP-ribose) Polymerase-1 Inhibition on the proliferation of Murine Colon Carcinoma CT26 Cells. Pathol Oncol Res 2009;15:323-328.
22 Garcia S, Bodano A, Gonzalez A, Forteza J, Gomez-Reino JJ, Conde C: Partial protection against collagen antibody-induced arthritis in PARP-1 deficient mice. Arthritis Res Ther 2006;8:R14-22.
23 García S, Bodaño A, Pablos JL, Gómez-Reino JJ, Conde C: Poly(ADP-ribose)polymerase inhibition reduces tumor neceosis factor-induced inflammatory response in rheumatoid synovial fibroblasts. Ann Rheum Dis 2008;67:631-637.
24 Cuzzocrea S, Genovese T, Mazzon E, Crisafulli C, Min W, Di Paola R, Muia C, Li JH, Esposito E, Bramanti P, Xu W, Massuda E, Zhang J, Wang ZQ: Poly(ADP-Ribose) Glycohydrolase Activity Mediates Post-Traumatic Inflammatory Reaction after Experimental Spinal Cord Trauma. J Pharmacol Exp Ther 2006;319:127-138.
25 Frizzell KM, Gamble MJ, Berrocal JG, Zhang T, Krishnakumar R, Cen Y, Sauve AA, Kraus WL: Global analysis of transcriptional regulation by poly(ADP-ribose) polymerase-1 and poly(ADP-ribose) glycohydrolase in MCF-7 human breast cancer cells. J Biol Chem 2009;284:33926-33938.
26 Erdélyi K, Bai P, Kovács I, Szabó E, Mocsár G, Kakuk A, Szabó C, Gergely P, Virág L: Dual role of poly(ADP-ribose) glycohydrolase in the regulation of cell death in oxidatively stressed A549 cells. FASEB 2009;23:3553-3563.
27 Li B, Cheung PY, Wang X, Tsao SW, Ling MT, Wong YC, Cheung AL: Id-1 activation of PI3K/Akt/NF-κB signaling pathway and its significance in promoting survival of esophageal cancer cells. Carcinogenesis 2007;28:2313-2320.
28 Lin L, Li J, Wang YL, Lin X: Relationship of PARG with PARP, VEGF and b-FGF in colorectal carcinoma. Chin J Cancer Res 2009;21:135-141.
29 Hao LX, Wang YL, Cai Li, Li YY: Inhibitory effect of 5-aminoisoquinolinone on PARP activity in colon carcinoma cell line HT-26. Chin J Cancer Res 2007;26:566-571.
30 Karin M, Cao Y, Greten FR, Li ZW: NF-κB in cancer from innocent bystander to major culprit. Nat Rev Cancer 2002;2:301-310.
31 Kovacs K, Toth A, Deres P, Kalai T, Hideg K, Gallyas F Jr, Sumegi B: Critical role of PI3-kinase/Akt activation in the PARP inhibitor induced heart function recovery during ischemia-reperfusion. Biochem Pharmacol 2006;71:441-452.
32 Tapodi A, Debreceni B, Hanto K, Bognar Z, Wittmann I, Gallyas F Jr, Varbiro G, Sumegi B: Pivotal role of Akt activation in mitochondrial protection and cell survival by poly(ADP-ribose)polymerase-1 inhibition in oxidative stress. J Biol Chem 2005;280:35767-35775.
33 Bar-shaiM, Carmeli E, Reznick AZ: The role of NF-κB in protein breakdown in immobilization, aging, and exercise from basic processes to promotion of health. Ann NY Acad Sci 2005;1057:431-447.
34 Cai D, Frantz JD, Tawa NE, Melendez PA, Oh B-C, Lidov HGW, Hasselgren P-O, Frontera WR, Lee J, Glass DJ, Shoelson SE: IKKβ-NF-κB activation causes severe muscle wasting in mice. Cell 2004;119:285-298.
35 Li M, Treadgill MD, Wang YL, Li C, Xiao L: Poly(ADP-Ribose) Polymerase Inhibition Down-Regulates Expression of Metastasis-Related Genes in CT26 Colon Carcinoma Cells. Pathobiology 2009;76:108-116.
36 Xian L, Guang-jie D, Wang YL, Fauzee NJ: Expressions of Poly (ADP-ribose) Glycohydrolase and membrane Type I Matrix Metalloproteinase (MT1-MMP) in Colorectal Carcinoma. Chin J Cancer Res 2010;22:186-193.
37 Bushdid PB, Chen CL, Brantley DM, Yull F, Raghow R, Kerr LD, Barnett JV: NF-κB mediates signal regulation of msx-1 expression. Dev Biol 2001;237:107-115.
38 Fauzee NJS, Pan J, Wang YL: PARP and PARG Inhibitors-New Therapeutic Targets in Cancer Treatment. Pathol Oncol Res 2010;16:469-478.
39 Asano T, Yao Y, Zhu J, Li D, Abbruzzese JL, Reddy SA: The PI 3-kinase/Akt signaling pathway is activated due to aberrant Pten expression and targets transcription factors NF-kappaB and c-Myc in pancreatic cancer cells. Oncogene 2004;23:8571-8580